JOURNAL OF MATERIALS SCIENCE 25 (1990) 5248–5256

Tellurium embrittlement of Type 316 steel

J. A. HEMSWORTH, M. G. NICHOLAS, R. M. CRISPIN
Materials Development Division, Harwell Laboratory, Oxfordshire, UK

The effect of molten tellurium and tellurium/caesium mixtures on the mechanical properties of Type 316 steel have been assessed at temperatures between 460 and 800° C using slow and fast strain rates. Tellurium embrittled the steel at temperatures above 600° C and this was associated with extensive chemical interaction and grain boundary penetration. At 600° C, the addition of even 2% of caesium caused tellurium to embrittle the steel severely. Similarities to zinc embrittlement exist that suggest tellurium also degrades by a two step process, with cracks being initiated due to the chemical interaction but propagating because of surface energy reductions.

1. Introduction

The mechanical integrity of fuel pin cladding is of crucial importance for the safe and efficient operation of nuclear reactors, and vast efforts have been devoted to the development of satisfactory materials and fabrication routes for major reactor systems. For fast reactors, austenitic stainless steels are the preferred cladding materials, and 20% cold worked Type 316 steel is that used for the UKAEA Prototype Fast Reactor at Dounreay in Scotland. The steel has to be mechanically stable in a demanding thermal and chemical environment, able to withstand external contact with the molten sodium coolant and internal contact with UO_2 fuel and arising fission products.

Potentially degrading interactions of concern include the so-called fuel-cladding chemical interaction (FCCI) which has caused low temperature intergranular failures [1]. Adamson and his co-workers [2–4] in the USA have associated this type of failure with the combined effects of stress and contact with molten fission products, specifically suggesting liquid metal embrittlement (LME) by molten tellurium–caesium mixtures as the damaging process. The tellurium was regarded as the actual embrittling agent, with the caesium fluxing the surface to promote wetting and providing a fast transport route [4].

These conclusions about tellurium were based on the crushing characteristics of slices cut from thin walled tubes, but most reported observations of LME have been made during tensile tests. These have shown that LME differs from other mechanical degradation processes such as stressed corrosion cracking or hydrogen embrittlement in that it apparently need not involve any chemical interaction [5]. Thus cracks can propagate rapidly, at speeds of m sec^{-1}, whenever the environment and stress levels permit a crack to nucleate, and there need not be any detectable chemical precursor stage whose progress can be monitored. In practice many liquid metal–solid metal systems do react chemically and this may play a role in the embrittlement process, as for the zinc–austenitic steel system during the Flixborough disaster [6], but this is not always so as demonstrated by recent work with the lithium–nickel system [7]. Therefore the potential severity and unpredictability of LME makes it important to have relevant experimental data before drawing conclusions about its technical significance in particular applications such as reactor operation. In this study, tensile test pieces of 20% cold worked Type 316 steel were exposed to molten tellurium or tellurium–caesium mixtures while being strained to destruction at various rates and temperatures. The tests were designed to establish whether any degradation observed exhibited the characteristics of LME.

2. Materials and methods

The steel used in this work was obtained from Fox Wire Ltd of Sheffield as 8 and 25 mm diameter cold drawn rods. In the as-received condition, its hardness was 248 HB, its proof stress was 712 MPa, its ultimate tensile strength (UTS) was 843 MPa, its elongation to failure (E_f) was 25% and its reduction in area was 69%. Its composition, summarized in Table I, conformed to BS 970: Part 4: 1970 316S16. Both the tellurium and the caesium were obtained from Koch Light Ltd of Haverhill, the tellurium as lump material with a purity of 99.999% and the caesium (which melts at 29° C) as 99.98% pure material contained in ampoules.

Two environments were used in the mechanical testing of the steel; argon and liquid metals. The tests in argon provided control data while those in the liquid metals were designed to provide evidence or otherwise of LME. Embrittlement can occur only if the liquid metal is in contact with the stressed solid, and hence preliminary experiments were conducted to define the wetting behaviour between tellurium and the steel. These tests used the sessile drop technique in which a small volume of tellurium was melted on a

TABLE I Steel composition (wt %)

Cr	Ni	Mo	Mn	Si	C	P	S	Fe
16.8	11.9	2.3	1.8	0.35	0.045	0.025	0.009	Remainder

0022–2461/90 $03.00 + .12

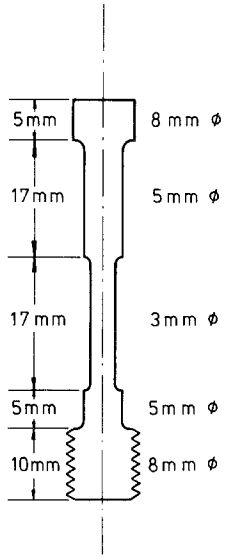

Figure 1 Tensile test piece used in this work.

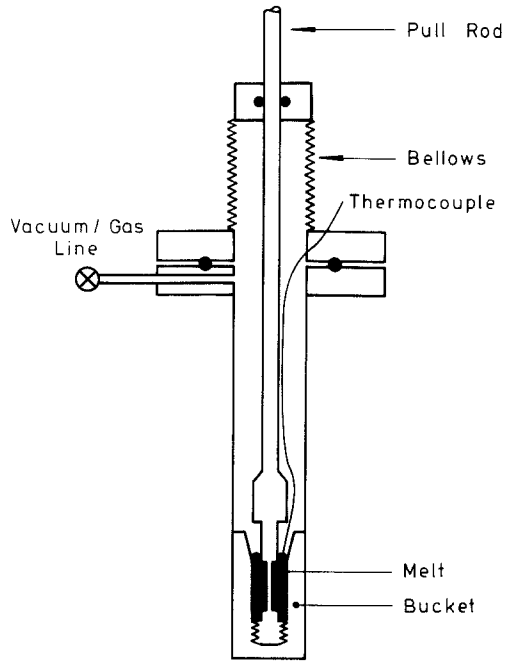

Figure 2 Schematic arrangement of the tensile test assembly.

horizontal steel disc cut from the 25 mm diameter rod. If the liquid spread out over the solid, wetting had occurred and contact had been achieved. To observe and record the melting behaviour a small vacuum furnace with diametrically opposed viewing ports was used, the furnace being backfilled with argon before power was supplied to melt the tellurium. In these tests, the tellurium appeared to melt at 455–458° C – the true temperature is 451° C, so either the measuring thermocouple was slightly misplaced or the samples exhibited some thermal lag – and spread out over the steel instantaneously, demonstrating excellent wetting.

Having confirmed the feasibility of stressing the steel in direct contact with tellurium, tensile test pieces of the type shown in Fig. 1 were prepared from the 8 mm diameter rods. Care was taken to ensure that the diameter of the gauge section was within the range 2.900 to 3.005 mm and that the length was between 16.9 and 17.1 mm. Changes of section radii were 1 mm and the surface of the gauge section was machined to a finish of no worse than 0.2 μm R_a. These tensile test samples were screwed into buckets made from the 25 mm diameter steel rods and then loaded into the bottom parts of tensile testing capsules made from AISI 321 steel, as sketched in Fig. 2. The bucket is locked into the bottom of the capsule by a bayonet arrangement that is not shown.

In control tests using an argon environment, the top and bottom halves of the capsule were sealed and then it was evacuated and filled with purified argon. In tests using liquid metal environments, the top and bottom halves of the capsule were posted into a high integrity steel bodied glove box filled with argon purified to less than 1 ppm of oxygen or water. Small lumps of tellurium were placed in the bucket and the capsule was sealed. In some experiments, a small quantity of caesium was added to the tellurium before the capsule was sealed. In both cases sufficient material was added to ensure that the gauge section and the greater part of the upper shoulder of the tensile test piece would be immersed when the tellurium or tellurium plus caesium melted.

The loaded capsule was posted out of the glove box and attached underneath the moveable crosshead of an Instron 1195 tensile test machine. The capsule pull rod passed through the moveable crosshead and was connected with the fixed top crosshead by an extension rod. A muffle furnace was slid over the bottom part of the capsule once a water cooled collar had been attached to protect the O-ring seals. The tensile test pieces were heated to 460 to 850° C at about 10 K min^{-1} and stabilized to within 2° C of the target temperature for 10 min before being strained to failure at crosshead speeds of 0.05 or 1 mm min^{-1}. Load extension curves such as those in Fig. 3 were recorded and used to derive UTS and E_f values with estimated accuracies of $\pm$10 MPa and $\pm$1% respectively.

After the tensile tests, the capsules used with the liquid metals were reposted into the glove box and unloaded. Unlike previous work with alkali metal

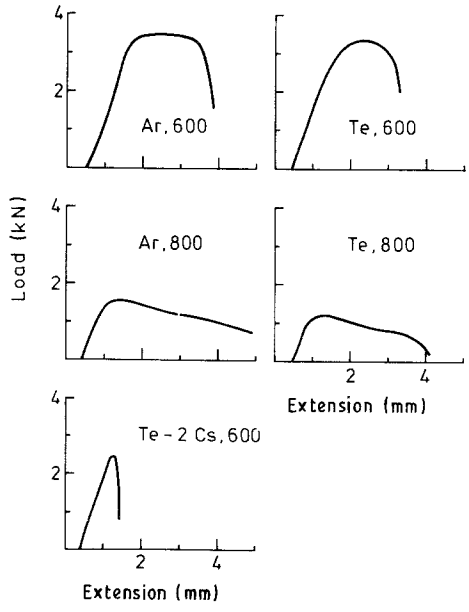

Figure 3 Load-extension curves for samples strained at 1 mm min^{-1}.

melts it was not practical to scour out the buckets, so a new one was used each time.

Subsequent to these tests, samples were cross-sectioned and examined using optical microscopy and, for some, electron probe microanalysis.

3. Results

Three series of experiments were performed to assess the effects on possible tellurium induced mechanical degradation of temperature, strain rate, and caesium additions. Each series was complemented by experiments performed in argon.

3.1. Effects of temperature

Tests were performed at temperatures ranging from 460 to 850° C using an extension rate of 1 mm min^{-1}, which corresponds to a strain rate of 1.1×10^{-3} sec^{-1}. The E_f and UTS values derived from these tests are presented in Table II and summarized in Fig 4.

Increasing the temperature caused a general enhancement of the ductility and loss of strength for samples tested in argon. The mechanical characteristics of the steel in tellurium and in argon were essentially the same at temperatures of 460 to 600° C, but at higher temperatures the use of tellurium environments caused both ductility and strength to be degraded. At temperatures of 650 to 850° C, the E_f values for samples tested in tellurium environments fell within the narrow range of 18 to 23%, while those for samples tested in argon increased from 20 to 68%. The differences in UTS values produced by changing to tellurium environments were less dramatic but still significant, the value at 850° C being decreased from 170 to 80 MPa.

Even the top parts of the tensile test samples which had been pulled out the molten tellurium when fracture occurred had solidified skulls of the metal attached to them. Thus it was not possible to examine the fracture faces directly, so the samples were cross-sectioned and examined microscopically. Low magnification examination showed that the samples tested at 650° C and below had failed by ductile tearing, but those tested at higher temperatures had fractured in a much more brittle manner, Fig. 5. All three micrographs shown in the figure exhibit signs that interaction with the tellurium melts had occurred and more detailed microscopy revealed something of the nature of the interactions. Thus a sample tested at 600° C formed a smooth fronted two layer interdiffusion zone at its surface and the solidified tellurium melt still attached was two phase, Fig. 6a. A similar structure was produced at 650° C, Fig. 6b, but there was also some evidence of grain-boundary grooving to create sharp notches. Contact with tellurium at 700° C produced a far more complex structure, Fig. 6c, with an

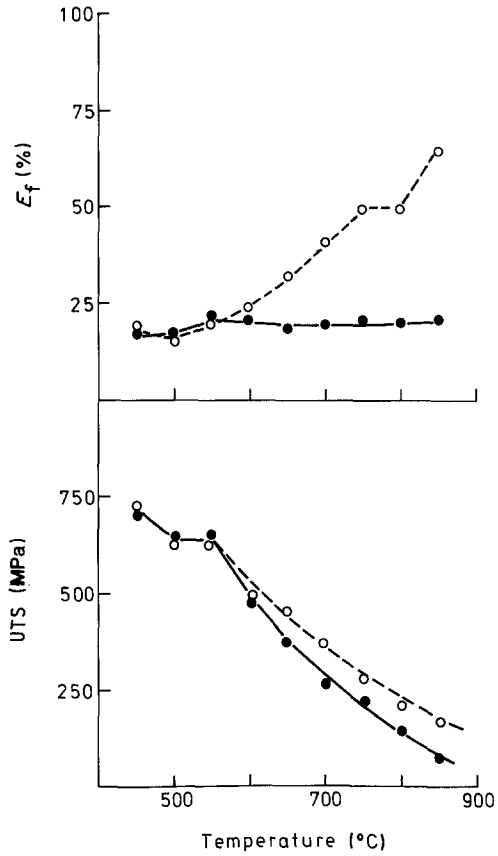

Figure 4 The effect of tellurium environments and test temperatures on the mechanical properties of samples stressed to destruction at a strain rate of 1.1×10^{-3} s^{-1}, ● – tellurium data, ○ – argon data.

TABLE II Mechanical properties in tellurium and argon environments

Temperature (° C)	Strain rate (sec^{-1})	Environment			
		Te		Ar	
		UTS (MPa)	E_f (%)	UTS (MPa)	E_f (%)
460	10^{-3}	710	16	730	18
500	10^{-3}	650	16	620	15
550	10^{-3}	650	25	630	20
600	10^{-3}	470	21	470	25
650	10^{-3}	380	18	450	33
700	10^{-3}	260	20	400	43
750	10^{-3}	220	22	270	50
800	10^{-3}	160	21	210	50
850	10^{-3}	80	23	170	68
600	5.5×10^{-5}	380	17	400	28
650	5.5×10^{-5}	250	21	280	41
700	5.5×10^{-5}	140	24	210	53
750	5.5×10^{-5}	70	15	80	38
800	5.5×10^{-5}	40	17	50	44

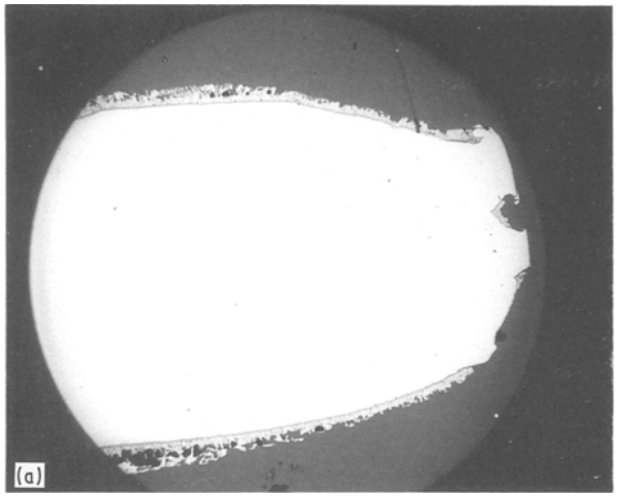

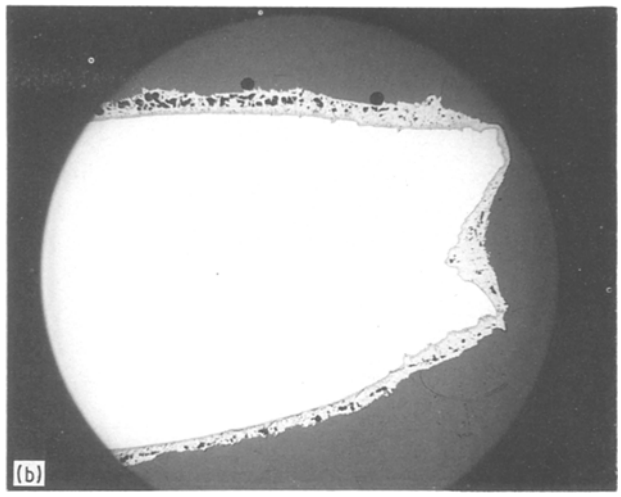

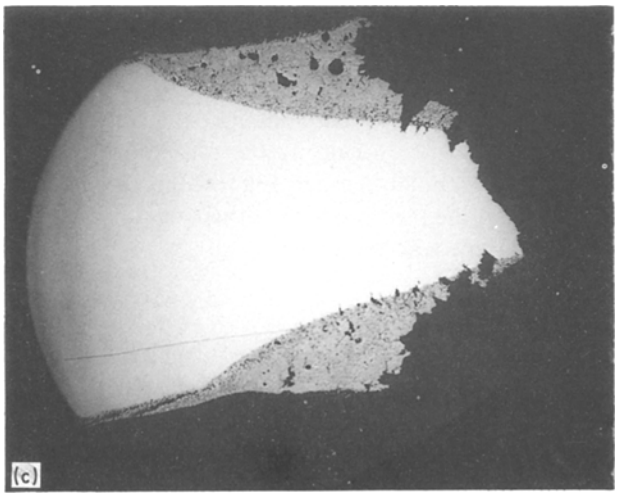

Figure 5 Cross sections through samples stressed to destruction in tellurium using a strain rate of $1.1 \times 10^{-3}\,sec^{-1}$ at (a) 600° C, (b) 650° C, (c) 700° C ×16.

irregular interaction front associated with grain-boundary voids in the steel. In that structure there was a similar tellurium zone voidage in the two phase adjacent to the steel.

3.2. Effects of strain rate

A second series of samples were tested to destruction in argon and in molten tellurium at temperatures of 600 to 800° C using a crosshead speed of 0.05 mm min^{-1}, which corresponds to a strain rate of $5.5 \times 10^{-5}\,sec^{-1}$. The mechanical data derived from the load–extension curves are summarized in Table II and plotted in Fig. 7.

As with the previous series of tests, the UTS values decreased progressively with temperature (and the use of tellurium environments caused some additional weakening). The ductility data were more complicated with the E_f values peaking at a test temperature of 700° C and then declining before starting to recover for tests conducted at 800° C. This behaviour was observed for tests performed in both argon and tellurium environments, but the use of tellurium rather than argon approximately halved the measured E_f values.

Comparison of the data for the first and second series of experiments, Fig. 8, shows effects of decreasing the strain rate to $5.5 \times 10^{-5}\,sec^{-1}$. There was no overall decrease in E_f values, the data from the slower strain rate tests oscillating about those from the first series of experiments. However, UTS values were consistently smaller for the slow strain rate tests. This reduction became more marked with temperature, rising from 20% at 600° C to 75% at 800° C.

Metallographic examination of cross-sectioned slow strain samples did not reveal any evidence of brittle failure akin to that shown in Fig. 5. At temperatures of 700° C or below, the tellurium had interacted to produce smooth interfaces between the steel and interdiffusion zones, Fig 9a. At 750° C and above, Fig. 9b, there was evidence of grain-boundary cracking but the microstructure was dominated by very thick (400μm or more) interdiffusion zones. At higher magnifications, Fig. 10, it was clear that grain boundaries were penetrated by tellurium at the higher temperatures.

A back-scattered electron image of the sample tip area shown in Fig. 9b showed that the thick interdiffusion zone comprised at least two regions, Fig. 11, and electron probe microanalyses surveys were used to derive elemental compositions across the area shown in Fig. 10. Considerable variations were found as summarized in Table III and illustrated in Fig. 12, the zones referred to being identified in Fig. 10. Chromium concentrations were enhanced in the interaction zone adjacent to the steel (Z1) but then decreased progressively as the sampled area was moved away from the steel. In contrast, the concentration of iron and nickel increased as the sampled area was moved away from the steel. Molybdenum was concentrated in one zone, Z2, while the tellurium contents of all the zones were high but decreased

TABLE III Compositions across the interdiffusion structure shown in Fig. 10, a sample strained at $5.5 \times 10^{-5}\,sec^{-1}$ and 750° C

Zone	Element (wt %)				
	Te	Fe	Cr	Ni	Mo
Z1	73	9	18	< 1	< 1
Z2	68	11.3	14.5	< 1	6.1
Z3	67	21	9	< 1	< 1
Z4	63	30	3	4	< 1

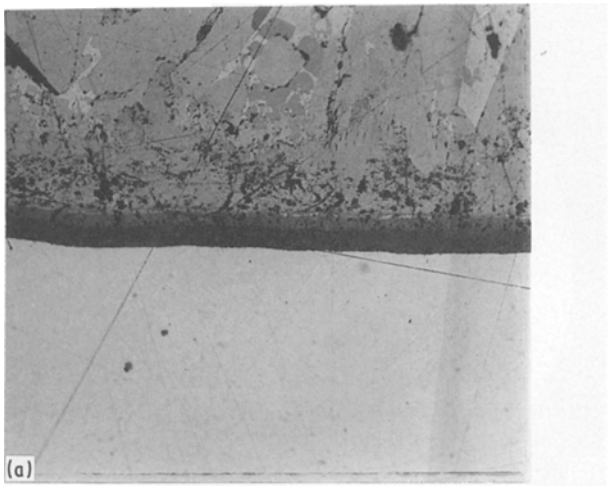

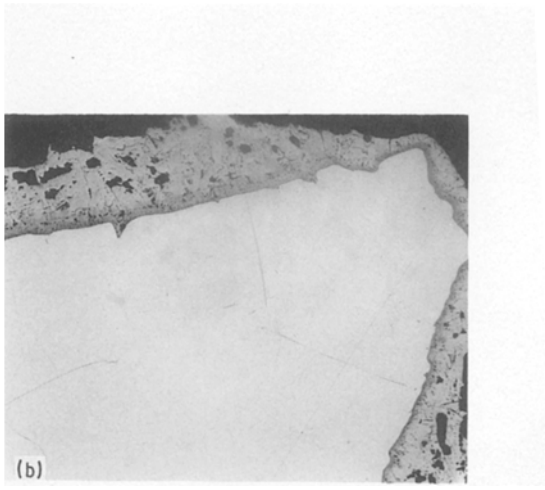

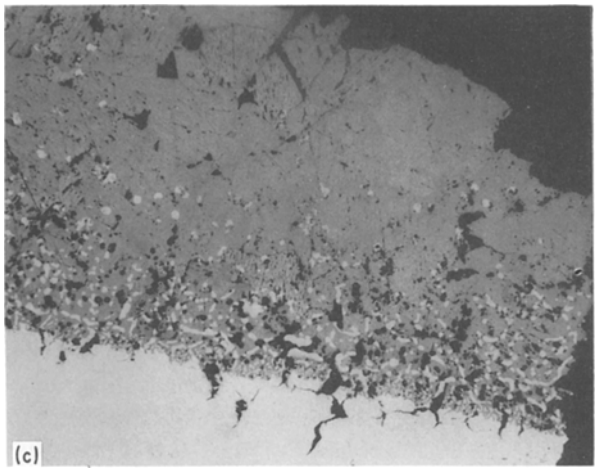

Figure 6 Cross sections through samples that had been stressed to destruction in tellurium using a strain rate of $1.1 \times 10^{-3}\,sec^{-1}$ at (a) 600° C, × 358, (b) 650° C. × 51 and (c) 700° C, × 132.

slightly from 73 to 63% as the sampled area was moved from the steel. Electron probe microanalyser surveys of samples tested at lower temperatures were more cursory but revealed the same general pattern, including the presence of a molybdenum rich zone.

3.3. Effects of caesium additions

Samples stressed to destruction at 600° C using a strain rate of $1.1 \times 10^{-3}\,sec^{-1}$ showed that the addition of caesium to tellurium had a marked effect on mechanical property data. The UTS and E_f values summarized in Table IV and plotted in Fig. 13 show that the introduction of caesium had a markedly detrimental effect. Introducing even 2% of caesium decreased the UTS of the steel to 350 MPa from 470 MPa in pure tellurium and argon, while the E_f fell to 6% as compared to 21% in tellurium and 25% in argon. Further significant degradation did not occur until the caesium content exceeded 20%.

TABLE IV Mechanical properties in Te–Cs melts. Samples stressed at 600° C using a strain rate of $1.1 \times 10^{-3}\,sec^{-1}$

Cs concentration (wt %)	UTS (MPa)	E_f (%)
0	470	21
2	350	6
4	340	6.3
10	350	5
20	370	6.5
30	110	2.3

The introduction of caesium also affected the fracture mode, even 2% causing the sample to fail in a brittle intergranular manner, Fig. 14. It is also notable that little of the melt remained attached and solidified on the sample fracture faces.

4. Discussion

This study has confirmed that molten tellurium and tellurium-caesium mixes can have a very detrimental effect on the mechanical properties of Type 316 austenitic steel. Previous evidence [4] related to tests with thin walled tubes which could have been weakened by

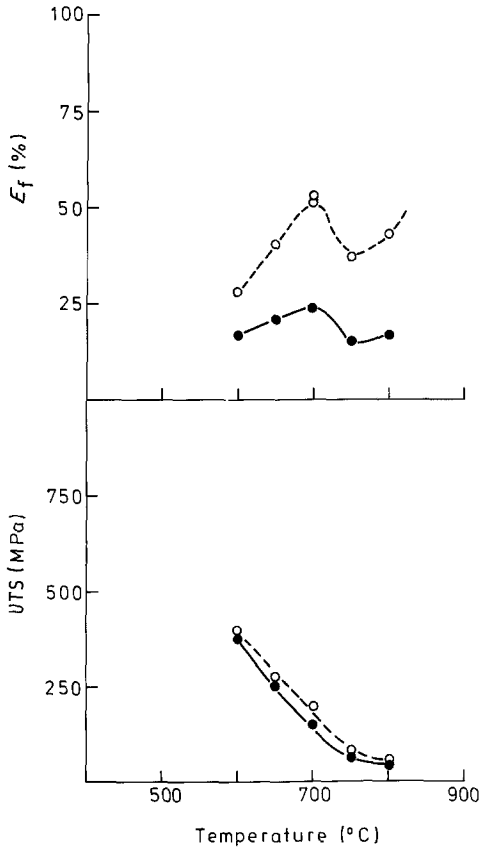

Figure 7 The effect of tellurium environments and test temperatures on the mechanical properties of samples stressed to destruction at a strain rate of $5.5 \times 10^{-5}\,sec^{-1}$. (●) tellurium, (○) argon.

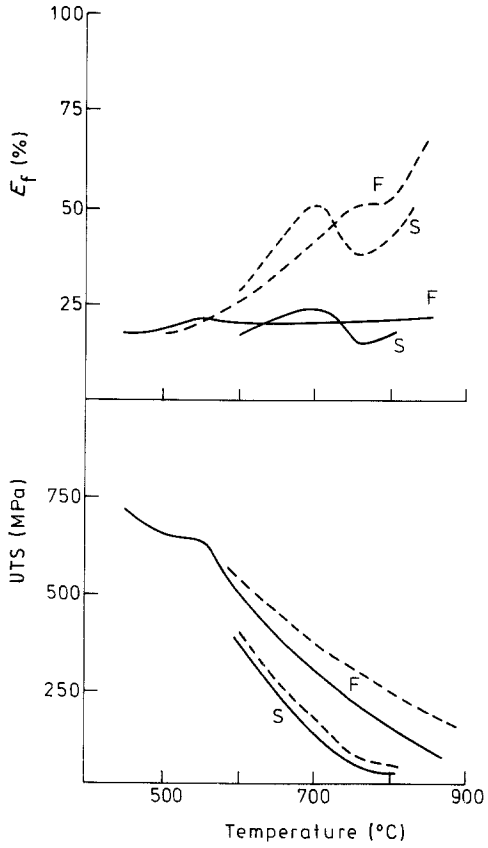

Figure 8 Comparison of mechanical property data for samples tested at strain rates of 1.1×10^{-3} (F) and $5.5 \times 10^{-5}\,\text{sec}^{-1}$ (S). (——) Te; (– – –) Ar.

corrosive wastage, but the present work was conducted with relatively substantial, 3 mm diameter, tensile test pieces and hence the results enhance the argument that the bulk mechanical degradation was induced by a surface damage event that propagated.

One mechanism that involves propagation of surface nucleated damage events in liquid metal environments is LME, and Adamson and his co-workers [2–4] concluded that tellurium induced embrittlement is indeed LME. This may be valid but some of our observations are not consistent with simple LME models [5]. These regard LME as a form of brittle fracture which is promoted by the liquid metal environment decreasing the surface energy of the solid and hence the work required for crack formation, as illustrated in Fig. 15. These models predict that embrittlement will be more severe at high strain rates and that ductility will decrease at a well defined temperature, such as the melting point of the embrittler, and be regained at some higher temperature. Our experimental observations, however, do not support either expectation. Further, empirical correlations associate severe LME with systems that have very limited solubilities and do not form intermediate compounds, but the interdiffusion and chemical interactions observed between tellurium and the steel were very marked.

While some of our observations were not in accord with expectations based on simple LME models, others were. Thus molten tellurium wetted the steel very well and will have decreased the surface energy of the steel, but it is difficult to predict by how much. The surface energy of the steel will be in the range 1.5 to $2.0\,\text{J m}^{-2}$ while that of the molten tellurium is $0.18\,\text{J m}^{-2}$ [8], and hence perfect wetting (a θ value of 0° as illustrated in Fig. 15) would require a surface energy reduction of no more than about 10%. However, the decrease could be more at temperatures above 600° C and evidence of this is provided by some of the microstructures. Grain-boundary grooving can be observed in Fig. 6b for a sample tested at 650° C. For cubic metals, the energy of the grain boundary is about a third of the surface energy, say $0.6\,\text{J m}^{-2}$ for our steel, and assigning a value of 60° for the dihedral angle, identified as ϕ in Fig. 15, leads to a predicted value of $0.35\,\text{J m}^{-2}$ for a steel surface in contact with tellurium (a decrease of 80%). Even larger decreases are implied by the filigree penetration of grain boundaries shown in Fig. 9 for a sample tested at 750° C. Tellurium therefore could produce major decreases in the surface energy contribution to crack propagation at high temperatures.

Adamson and his co-workers [4] claimed that the presence of caesium was a necessary precondition for tellurium embrittlement at about 600° C. While this work has shown that conclusion to be invalid at high temperatures, it has also shown that caesium can

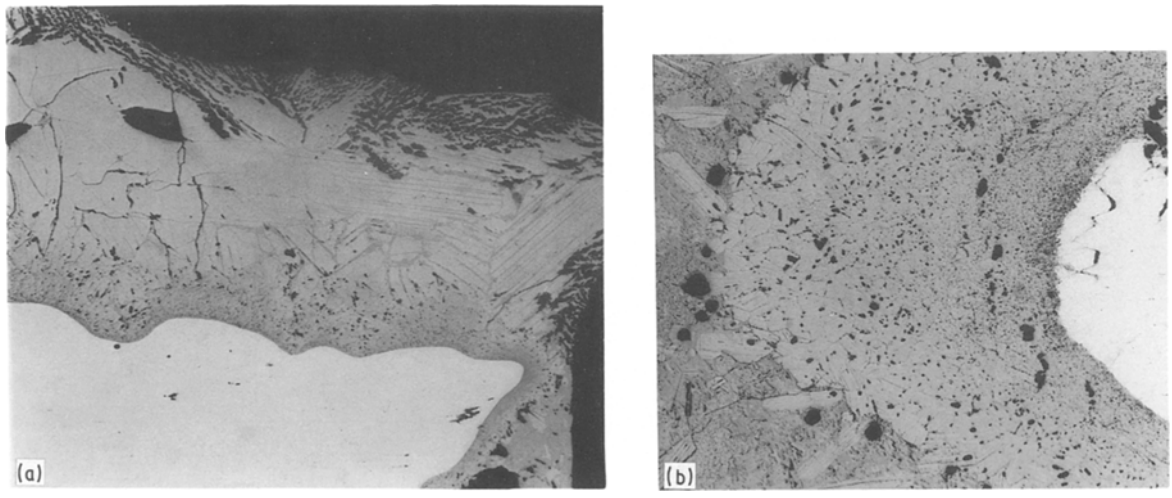

Figure 9 Cross sections through samples stressed to destruction in tellurium using a strain rate of $5.5 \times 10^{-5}\,\text{sec}^{-1}$, (a) 700° C, ×66, (b) 750° C, ×66.

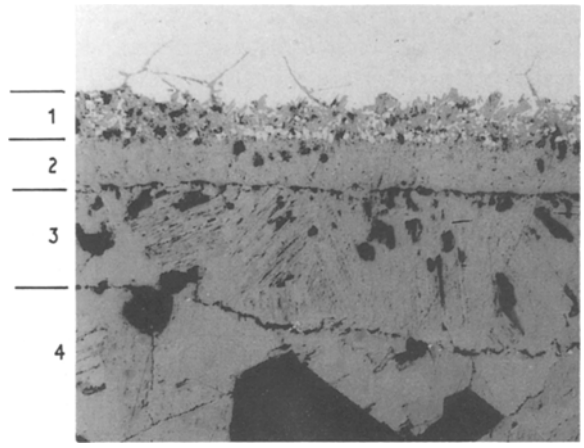

Figure 10 Cross section through a sample stressed to destruction at 750° C using a strain rate of $5.5 \times 10^{-5}\,\text{sec}^{-1}$, × 331.

promote embrittlement at temperatures of 600° C. Only 2% of caesium was needed to cause a marked decrease in both ductility and strength, Fig. 13, so the additive must have segregated quite strongly to the steel-melt interface. Its effect on the surface energy has not been measured and cannot be predicted readily, but some guidance can be derived by assuming the local concentration of caesium approached 100%. The energy of an iron surface in contact with sodium at its melting temperature has been calculated as $1.3\,\text{J m}^{-2}$ by Miedema and den Broeder [9], and the energy of a surface in contact with caesium should be similar since the heats of solution of iron in sodium and caesium are very close [10]. Strong segregation of caesium to the steel–melt interface, therefore, could triple the surface energy decrease caused by tellurium at 600° C and make crack propagation easier. This argument implies that caesium is the active species in crack propagation and not a mere fluxing agent [2].

So far, the effects of liquid metal environments on crack propagation have been discussed, but first the crack must nucleate. Models of non-reactive crack nucleation are still being developed, but in practice it has been observed that chemical interaction to form brittle intermetallic layers can play a role for important technical systems. Thus for the zinc–austenitic steel system it was found that an incubation period occurred prior to the propagation of cracks and this was associated with diffusion along grain boundaries

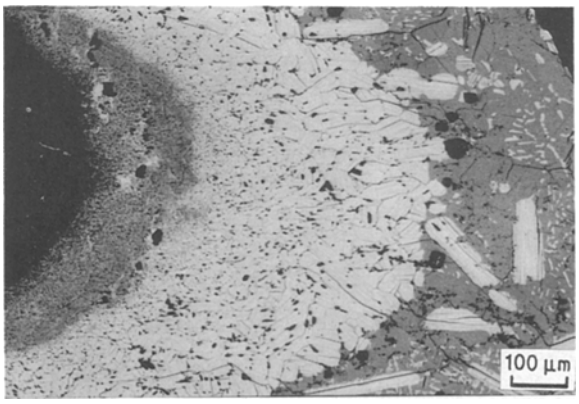

Figure 11 Backscattered electron image of the area shown in Fig. 9(b) revealing atomic number variations, × 69.

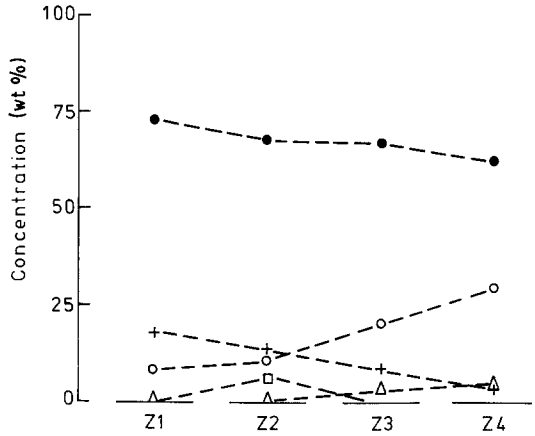

Figure 12 Composition variations across the four zones of the area shown in Fig. 10. (●) Te, (○) Fe, (+) Cr, (△) Ni, (□) Mo.

to produce a nickel denuded zone that transformed to ferrite, generating severe local volume mismatch stresses [11]. With the zinc–austenitic steel system, embrittlement is severe only at temperatures of about 750° C and above when grain boundary diffusion becomes dominant.

Tellurium penetration of grain boundaries can be associated also with the conditions that caused embrittlement, Figs 6 and 10. The temperatures for the onset of embrittlement are similar to those for zinc, and tellurium forms intermetallic compounds with iron, nickel, chromium and molybdenum [12]. The stabilities of some of these compounds change as the temperature is increased to the range in which embrittlement is observed, but whether a nucleation process occurs that is similar to that observed with zinc is not known. However it may be significant that molybdenum is locally concentrated in the inter-diffusion zone since the dissolution of molybdenum carbides in the grain boundaries could render crack propagation easier.

This work has provided additional evidence about the detrimental effects of molten tellurium on the mechanical properties of Type 316 austenitic steel and

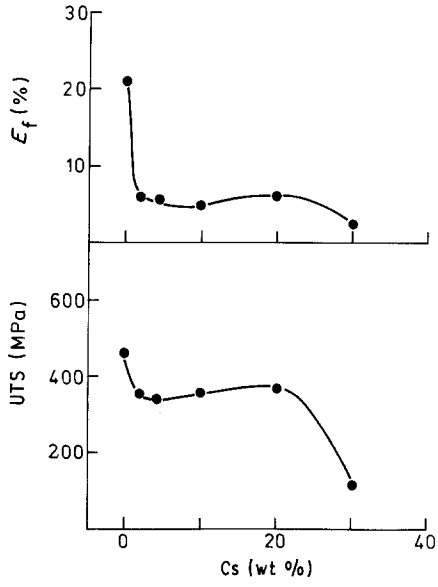

Figure 13 The effect of caesium additions on the mechanical properties of steel stressed to destruction in tellurium melts at 600° C using a strain rate of $1.1 \times 10^{-3}\,\text{sec}^{-1}$.

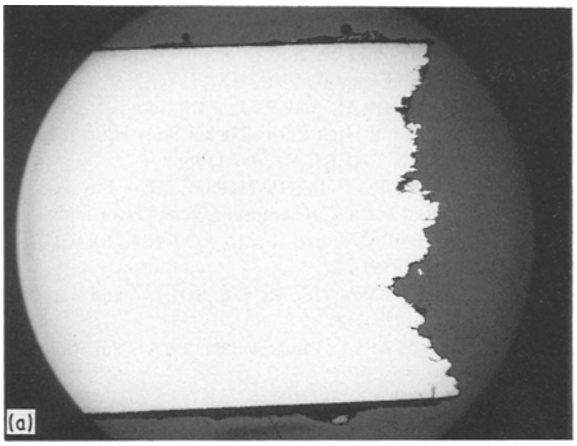

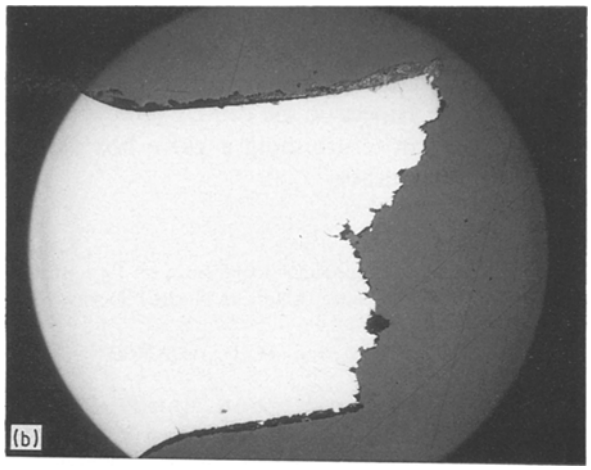

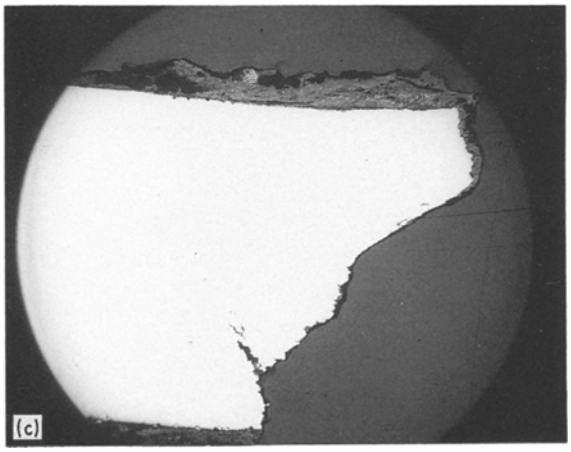

Figure 14 Cross sections through samples that had been stressed to destruction in tellurium–caesium melts; (a) 2% Cs (b) 4% Cs (c) 10% Cs, × 16.

the influence of alloying the tellurium with caesium. Compared with the work of Adamson and his colleagues, a wider temperature range has been used and effects of low concentrations of caesium have been evaluated. Semantically, the degradation must be liquid metal embrittlement, but the actual mechanics are complex. While arguments can be advanced that crack propagation can be driven by surface energy decreases, the nucleation process is not clear except for being associated with tellurium–steel interactions. Thus of the degradation of fuel pin cladding will be influenced, perhaps crucially, by the rates at which tellurium fission products can be transported to the cladding and the thermodynamic activity of the tellurium in the fission product melts.

5. Conclusions

1. Tellurium embrittles Type 316 austenitic steel at temperatures above 600° C.

2. The addition of caesium to tellurium is not necessary to ensure high temperature embrittlement, but even 2% caesium promotes embrittlement at 600° C.

3. Tellurium reacts vigorously with Type 316 steel to produce multilayered interdiffusion zones, with molybdenum being concentrated in one layer.

4. The embrittlement mechanism is complex, but crack nucleation could be associated with the formation of brittle intermetallic compounds and crack propagation with large decreases in the surface energy of the steel caused by contact with the tellurium.

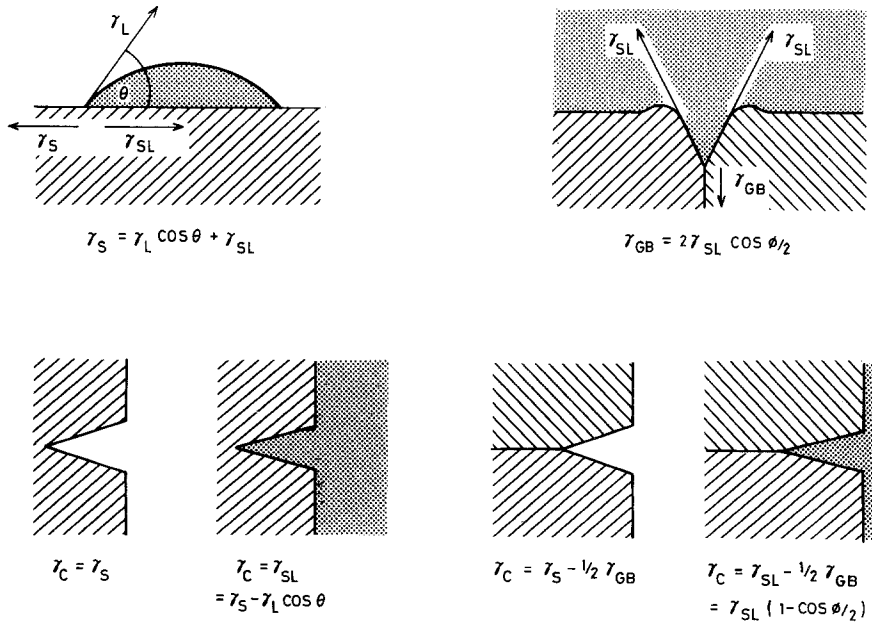

Figure 15 Energy values in liquid metal embrittlement. The symbol γ denotes an energy per unit area, and the suffices identify: C the crack surface; S the solid metal surface; SL the solid–liquid interface; GB the grain boundary; and L the liquid metal surface.

Acknowledgements

This work was conducted as part of the UKAEA underlying programme on fracture studies. The work of Mr R. W. M. Hawes on the EPMA surveys and of Mr R. A. Airey in refurbishing a glove box was of great help to the authors.

References

1. K. Q. BAGLEY, Proceedings Conference on Fast Breeder Reactor Fuel Performance, American Nuclear Society, 1979, p. 233.
2. S. VAIDYANATHAN and M. G. ADAMSON, *Trans. ANS*, **38** (1981) 262.
3. M. G. ADAMSON and W. H. REINEKING, in "Embrittlement by Liquid and Solid Metals", Conference Proceedings, AIME (1984), edited by M. H. Kamdar, p. 523.
4. M. G. ADAMSON, E. A. AITKIN and S. VAIDYANATHAN, *Nature* **295** (1982) 49.
5. N. S. STOLOFF, in "Embrittlement by Liquid and Solid Metals," Conference Proceedings, AIME (1984), edited by M. H. Kamdar, p. 1.
6. "The Flixborough Disaster", Report of Court of Inquiry, Department of Employment, HMSO (1975).
7. M. G. NICHOLAS and P. J. FERNBACK, "Some Tensile Properties of High Purity Nickel Stressed in Alkali Metal Environments", AERE-R13057 (1988).
8. T. IIDA and R. I. L. GUTHRIE, "The Physical Properties of Liquid Metals" (Clarendon Press, Oxford, 1988) p. 134.
9. A. R. MIEDEMA and F. J. A. DEN BROEDER, *Z. Metall.* **70** (1979) 14.
10. A. R. MIEDEMA, F. R. DE BOER and R. BOOM, *Calphad* **1** (1977) 341.
11. A. H. COTTRELL and P. R. SWANN, *Chem. Eng.* (1976) 266.
12. T. B. MASSALSKI, "Binary Alloy Diagrams," (American Society of Metals, Metals Park, Ohio, 1986).

Received 11 July
and accepted 12 December 1989